Statistics of resonances and delay times in random media: beyond random matrix theory

2005 J. Phys. A: Math. Gen. 38 10761

(http://iopscience.iop.org/0305-4470/38/49/018)

INSTITUTE OF PHYSICS PUBLISHING JOURNAL OF PHYSICS A: MATHEMATICAL AND GENERAL

J. Phys. A: Math. Gen. **38** (2005) 10761–10786 doi:10.1088/0305-4470/38/49/018

Statistics of resonances and delay times in random media: beyond random matrix theory

Tsampikos Kottos

Department of Physics, Wesleyan University, Middletown, CT 06459-0155, USA
and
Max-Planck-Institute for Dynamics and Self-Organization, Bunsenstrasse 10,
D-37073 Göttingen, Germany

Received 29 July 2005, in final form 5 October 2005
Published 22 November 2005
Online at stacks.iop.org/JPhysA/38/10761

Abstract

We review recent developments in quantum scattering from mesoscopic systems. Various spatial geometries whose closed analogues show diffusive, localized or critical behaviour are considered. These are the features that cannot be described by the universal random matrix theory results. Instead, one has to go beyond this approximation and incorporate them in a non-perturbative way. Here, we pay particular attention to the traces of these non-universal characteristics, in the distribution of the Wigner delay times and resonance widths. The former quantity captures time-dependent aspects of quantum scattering while the latter is associated with the poles of the scattering matrix.

PACS numbers: 03.65.Nk, 05.45.Mt

(Some figures in this article are in colour only in the electronic version)

1. Introduction

Quantum mechanical scattering in systems with complex internal dynamics has been a subject of intensive research activity for a number of years. This interest was motivated by various areas of physics, ranging from nuclear [1], atomic [2] and molecular [3] physics, to mesoscopics [4], quantum chaos [5, 6] and classical wave scattering [7, 8]. Recently, the interest in this subject was renewed due to technological developments in quantum optics associated with the construction of new types of lasers [9, 10] and experimental investigation of atoms in optical lattices [11].

The most fundamental object characterizing the process of quantum scattering is the unitary S-matrix relating the amplitudes of incoming waves to the amplitudes of outgoing waves. The recent advances in mesoscopic physics and quantum chaos led to a fast development of powerful theoretical techniques which allow us to understand the statistical properties of the S-matrix. At present, there are two complementary theoretical tools employed

to calculate statistical properties of the S-matrix, namely the semiclassical and the stochastic approach. The starting point of the first is a representation of the S-matrix elements in terms of a sum of classical orbits [5, 6] while the latter exploits the similarity with ensembles of random matrices [12]. At the same time, recent experimental progress allowed a direct comparison of the theoretical predictions with actual experimental results. Microwave experiments (see [13, 14] and references therein) offer a unique possibility of checking even details of the existing theories in cases where this is hardly possible by other methods, while they raise new challenging questions (see, for example, [13–15]).

Apart from the study of the distribution of the S-matrix elements, resonance widths and Wigner delay time distributions also gained much attention. The latter quantity captures the time-dependent aspects of quantum scattering. It can be interpreted as the typical time an almost monochromatic wave packet remains in the interaction region. Resonances are defined as poles of the S-matrix occurring at complex energies $\mathcal{E}_n = E_n - \frac{\mathrm{i}}{2}\Gamma_n$, where E_n is the position and Γ_n is the width of the resonance. They correspond to the 'eigenstates' of the open system that decay in time due to the coupling to the 'outside world' and they are related to conductance fluctuations and current relaxation [16]. For chaotic systems in the ballistic regime, random matrix theory (RMT) is applicable, and the distributions of resonance widths $\mathcal{P}(\Gamma)$ and Wigner delay times $\mathcal{P}(\tau)$ are known. A review of the RMT results can be found in [12] (see also [6]).

In this contribution, we aim at giving an overview of the recent developments in scattering from open samples in conditions where RMT is not applicable and deviations from 'universality' due to the appearance of localization are apparent. Although our presentation is focused on random media, one always has to keep in mind that these results are also valid for dynamical systems with chaotic classical limit. Despite the fact that these systems are deterministic (in contrast to random media where randomness is 'built up' with the system) localization occurs due to complicated interference effects created by the underlying classical chaotic dynamics, and for this reason it is termed *dynamical localization* [17].

The observables that will be in the focus of our presentation are the distributions of resonance widths and delay times. We consider various spatial geometries and models whose closed analogues show features such as diffusion, criticality or localization. A short overview of localization theory and the definitions of the various regimes are given in section 2. In section 3 we present the mathematical formalism associated with the scattering process, and define the quantities of interest. In section 4 we review the consequences of localization in the resonance width distribution. The corresponding results for the delay times are analysed in 5. Finally, in section 6 we present some results for quasi-periodic systems at criticality. Our conclusions are given in section 7.

2. Various regimes in localization theory: a brief overview

Localization of waves has always been among the most difficult yet most fascinating topics in the study of wave propagation in disordered media. The first studies dealt with infinite media, showing that localization is always achieved in one and two dimensions but that a minimum amount of disorder is required in dimensions larger than 2 [18–20]. Its main feature is that the eigenfunctions of a disordered medium in the localized regime are characterized by an exponential decay in space, i.e., $|\Psi_n(\mathbf{r})| \sim \exp(-|\mathbf{r} - \mathbf{r_0}|/\xi)$, where ξ is the localization length. A direct consequence is that transmission is inhibited and the system behaves as an insulator.

The fingerprints of localization in various quantities associated with the closed systems have been identified and quite well understood. Detailed numerical and theoretical studies

gave a clear picture how the statistical properties of these quantities change as the disorder strength increase (for a recent review, see [21] and references therein). Let us consider a quantum dot. For weak disorder, such that the mean free path l_{mean} is larger than the system size L, the dot can be considered clean and the dynamics across its length is *ballistic*. We will further assume that the 'cavity' defining the dot has an irregular shape and therefore the ballistic motion is chaotic. In these systems, the relevant time scale is the ergodic time τ_{erg}, which is of the order of the time of flight across the sample. The related energy scale is known as Thouless energy and it is given by $E_{\mathrm{Th}} = \hbar/\tau_{\mathrm{erg}}$. One can further define a dimensionless conductance as the ratio $g = E_{\mathrm{Th}}/\Delta$ where Δ is the mean level spacing. The condition $g \gg 1$ guarantees that a large number of internal modes are mixed by the chaotic scattering taking place at the irregular boundary. In the limit where $g \to \infty$, the predictions of random matrix theory (RMT) were shown to describe accurately the statistical properties of various observables related with the ballistic chaotic dot. For example, the eigenstates are extended all over the system, the eigenvalue spacing distribution follows, with a good accuracy, the famous Wigner surmise [22, 23] etc.

As the disorder increases the system becomes *diffusive*. This regime is characterized by the condition that the system size L is larger than the mean free path l_{mean} but still smaller than the localization length ξ, i.e., $l_{\mathrm{mean}} \ll L \ll \xi$. Using the powerful sigma-model approach it was explained how the deviations from the RMT results arise [21, 24]. Detailed numerical experiments [25–27] verified the theoretical predictions. These deviations are particularly strong at the far 'tails' of the distribution of the eigenfunction intensities as well as of some related quantities and are signatures of the underlying classical diffusive dynamics [25–27]. They were shown to be related to anomalously localized states termed *pre-localized* states. In [25, 26] it was found that pre-localized states are also present in quantum systems with deterministic chaotic dynamics. As far as the spectral correlations are concerned it has been shown that there are large deviations above the Thouless energy $E_{\mathrm{Th}} = \hbar/\tau_{\mathrm{Th}}$ where $\tau_{\mathrm{Th}} = \hbar D/L^2$ is the time to diffuse through the system with diffusion constant D [23, 29]. The Thouless conductance g is related to the latter as $g = DL^{d-2}$ where d is the dimensionality of the system. Rapid development in microwave techniques allowed for a direct observation of some of these predictions in microwave experiments [30–33].

The deviations of the level and eigenfunction statistics from their RMT form strengthen with increasing disorder and become especially pronounced in the *localization* regime . In this regime, inhibition of wave diffusion due to interference of multiple scattering waves takes place [18]. The resulting scenario depends strongly on the dimensionality of the sample and the disorder strength. It turns out that the eigenstates are exponentially localized in low-dimensional systems even for arbitrary weak disorder. As a matter of fact the localization regime is defined through the condition that $L < \xi$. One of the consequences following from this fact is the prediction that the conductance of a sample goes exponentially to zero with the increase in its length and the sample behaves as an insulator. In contrast, disordered single-particle systems in more than two dimensions exhibit a reacher behaviour. If the disorder is weak enough there is no localization and the system has a metallic behaviour while for strong disorder strength we recover the localization regime. The transition point from a metallic to localized behaviour is of special interest and is called metal–insulator transition (MIT).

The MIT where the phase transition from localized to extended states occurs is characterized by remarkably rich critical properties. In particular, the level spacing distribution acquires a scale-independent form [28] while other level statistical measures show distinct critical features [21, 29, 34]. At the same time, the eigenfunctions show strong fluctuations on all length scales and represent multi-fractal distributions [21, 24, 35–37]. As a matter of fact, a connection between multi-fractality and statistical properties of eigenvalues at MIT has

been recently established [34]. The multi-fractal structure of the eigenfunctions is usually quantified by studying the size dependence of the so-called participation numbers (PN)

$$\mathcal{N}_q = \left(\int |\psi(\mathbf{r})|^{2q} \, \mathrm{d}\mathbf{r} \right)^{-1} \propto L^{(q-1)D_q} \tag{1}$$

where L is the linear size of the system and D_q are the multi-fractal dimensions of the eigenfunction $\psi(\mathbf{r})$. Among all the dimensions, the correlation dimension D_2 plays the most prominent role. The corresponding PN is roughly equal to the number of nonzero eigenfunction components, and therefore is a good and widely accepted measure of the extension of the states. At the same time D_2 manifests itself in a variety of other physical observables. As examples, we mention the statistical properties of the spectrum [21, 34], the anomalous spreading of a wave packet, and the spatial dispersion of the diffusion coefficient [38].

At the same time a considerable effort was made to understand the shape of the conductance distribution $\mathcal{P}(g)$ at MIT [16, 39, 40]. However, it is still unclear whether the limiting $\mathcal{P}(g)$ is entirely universal, i.e., dependent only on the dimensionality and symmetry class, as required by the 1-parameter scaling theory of localization [20]. The latter is one of the major achievements in the long history of studying the MIT. Its basic assumption is that the change of the typical conductance g with the sample size L depends only on the conductance itself, and not separately on energy, disorder, size and shape of the sample, the mean free path etc.

Although many studies have been devoted to the analysis of eigenfunctions and eigenvalues and of conductance, the properties of resonances, and delay times were left unexplored until recently. Nevertheless, it was clear from the very beginning that their statistical properties depend strongly on the nature of the states of the finite system 'in isolation'. Thus Anderson localization must leave its fingerprints in these quantities which after all reflect the 'leakage' of the waves to the leads, through the sample boundaries. In the next sections, we will review the outcome of these studies and their deviations from the RMT predictions due to non-universal features.

3. Quantum scattering: basic concepts

The scattering S-matrix relates the outgoing wave amplitudes to the incoming wave amplitudes. Assuming M open channels, one can show that the $M \times M$ scattering matrix can be written in the form [1]

$$S(\mathcal{E}) = \mathbf{1} - 2\mathrm{i}\pi V^{\dagger} \frac{1}{\mathcal{E} - H_{\mathrm{eff}}} V \qquad H_{\mathrm{eff}} = H_0 - \mathrm{i}\pi V V^{\dagger}. \tag{2}$$

Here, H_0 stands for an N-dimensional self-adjoint Hamiltonian describing the closed counterpart of the system under consideration, $\mathcal{E}$ stands for the energy of the incoming waves, and V is an $M \times N$ operator that contains matrix elements coupling the internal motion to one of the open M channels. In principle, the matrix elements of the operator V depend on energy. However, since this dependence is very weak (far away from channel thresholds), we can ignore it and consider $V_{i,j}$ to be energy independent. $\mathbf{1}$ is the $M \times M$ unit matrix. For a detailed derivation of the scattering matrix for the case of a tight-binding model, see [41] while for a chaotic cavity, see [42]. It is easy to verify that form (2) ensures the unitarity of the scattering matrix, i.e., $S^{\dagger}S = \mathbf{1}$, provided the energy $\mathcal{E}$ takes only real values. When one allows the energy parameter to have a nonzero imaginary part, the S-matrix unitarity is immediately lost. Having $\mathrm{Im}\,\mathcal{E} > 0$ corresponds to the physical situation of uniform damping inside the system [8, 43] and it is responsible for the losses of the outgoing flux of the

particles as compared to the incoming flux. The 'dual' case $\mathrm{Im}\,\mathcal{E} < 0$ corresponds to uniform amplification. The balance between the two fluxes is precisely the physical mechanism behind the S-matrix unitarity.

The poles of the scattering matrix S are associated with the formation of resonance states. They represent long-lived intermediate states to which bound states of a closed system are converted due to coupling to continua. Due to causality, they are located in the lower half plane, i.e., $\mathcal{E}_n = E_n - \frac{\mathrm{i}}{2}\Gamma_n$, where E_n and Γ_n are the position and the width of the resonances, respectively. They are solutions of the following secular equation,

$$\det(\mathcal{E} - H_{\mathrm{eff}}(\mathcal{E})) = 0. \tag{3}$$

where the resonance width Γ is inversely proportional to the lifetime of the corresponding resonance state. From equations (2) and (3) it is clear that the formation of resonances is closely related to the internal dynamics inside the scattering region which is governed by H_0.

Another quantity that will be in the focus of this contribution is the Wigner delay time [44] and its variations (for an overview on the various definitions of delay times and their physical importance, see [45]). It captures the time-dependent aspects of quantum scattering. It can be interpreted as the typical time an *almost monochromatic* wave packet remains in the interaction region. Formally, the Wigner delay time τ_W is related to the energy derivative of the total phase of the unimodular S-matrix

$$\tau_W(E) = \frac{1}{M}\,\mathrm{Tr}\,Q(E), \qquad Q(E) = -\mathrm{i}\hbar S^{\dagger}(E)\frac{\mathrm{d}S(E)}{\mathrm{d}E} \tag{4}$$

where $Q(E)$ is called the Wigner–Smith time delay matrix [44]. Its eigenvalues τ_q are called proper delay times, and correspond to the time the particle dwells at a particular channel $q = 1, \ldots, M$. Alternatively, one can also define the *partial* delay times τ_q^{p} as the energy derivatives of the eigenphases $\{\theta_q\}, q = 1, \ldots, M$ of the unimodular S-matrix, i.e., $\tau_q^{\mathrm{p}} = \partial\theta_q/\partial E$ [12]. Beyond the one-channel case, proper and partial delay times differ, although the sum of partial/proper delay times over all M scattering channels is always equal and yields the Wigner delay time.

4. Resonances

In this section, we analyse the distribution of resonances $\mathcal{P}(\Gamma)$. The properties of resonances are of fundamental as well as technological interest. One can show that they determine the conductance fluctuations of a quantum dot in the Coulomb blockade regime [46], or the current relaxation. The latter study constitutes a fundamental source of physical information for systems which are coupled to a continuum via metallic leads or absorbing boundaries. While the radioactive decay is a prominent paradigm, more recent examples include atoms in optically generated lattices and billiards [47, 48], the ionization of molecular Rydberg states [49], photoluminescence spectroscopy of excitation relaxation in semiconductor quantum dots and wires [50], and pulse propagation studies with electromagnetic waves [51].

From the theoretical point of view, one can approach the problem of current relaxation by evaluating the survival probability $P(t)$ to remain inside the sample. For a narrow wave packet which is initially localized near the boundary of an open sample of volume Ω

$$P(t) = \int_{\Omega} |\Psi(t, \mathbf{r})|^2\,\mathrm{d}\mathbf{r} \sim \int_0^{\infty} \mathrm{d}\Gamma\,\Gamma\mathcal{P}(\Gamma)\exp(-\Gamma t). \tag{5}$$

The approximation above (modal approximation) is valid [21, 24, 51–55] for times larger than the Heisenberg time t_H and allows us to calculate a dynamical quantity such as $P(t)$, based on information about resonances. We note that sometimes it is instructive to represent

the obtained results (5) in terms of the superposition of simple relaxation processes with mesoscopically distributed relaxation times t_ϕ [21, 24]:

$$P(t) \sim \int \frac{\mathrm{d}t_\phi}{t_\phi} \mathrm{e}^{-t/t_\phi} \mathcal{P}(t_\phi). \tag{6}$$

The total current leaking out of the sample is then related to the survival probability by

$$J(t) = -\frac{\partial P(t)}{\partial t}. \tag{7}$$

The ability of constructing micro-lasers with chaotic resonators which produce high-power directional emission [9] as much as the experimental realizations of the so-called random lasers [10] where the feedback is due to multiple scattering within the medium (instead of being due to mirrors), is another reason why statistical properties of resonances became fashionable in our time. For the latter application, the knowledge of resonance width distribution can result in the knowledge of the statistical properties of the lasing threshold.

The lasing threshold is given by the value of the smallest decay rate (i.e., smallest resonance width) of all eigenmodes in the amplification window [56, 57]. The underlying reasoning is that in the mode with the smallest decay rate the photons are created faster by amplification than they can leave (decay) the sample. Assuming that the number of modes $K \gg 1$ that lie in the frequency window where the amplification is possible, has resonance widths Γ that are statistically independent, one gets for distribution of lasing thresholds $\tilde{\mathcal{P}}(\Gamma)$ [56–58],

$$\tilde{\mathcal{P}}(\Gamma) = K\mathcal{P}(\Gamma \ll 1)\left[1 - \int_0^\Gamma \mathcal{P}(\Gamma' \ll 1)\,\mathrm{d}\Gamma'\right]^{K-1} \tag{8}$$

where we have assumed that all K resonances are distributed according to $\mathcal{P}(\Gamma \ll 1)$. The validity of this approximation was verified recently in the framework of the RMT [59]. An important outcome of [25, 26] was that one can identify in diffusive systems traces of pre-localized states in the latter distribution and consequently in $\tilde{\mathcal{P}}(\Gamma)$. This might shed some light on recent experimental finding for random lasers which suggests the appearance of localized modes in diffusive samples [60]. We note that if these localized modes are indeed related to the pre-localized states then their size has to be much larger than the mean free path l_{mean} by the very nature of the non-linear sigma model which predicts them. Using this as a starting observation, it was suggested recently (see [61] and references therein) that these localized modes are related with the so-called 'almost localized states' supported by rare traps of sub-mean free path size. These latter solutions are very sensitive to the microscopic details of the system and thus are not universal as opposed to pre-localized states. Further research is needed in order to clarify this point.

4.1. Ballistic regime

For ballistic/chaotic systems, RMT modelling is applicable. Its main advantage is its universality. At the same time, universality means that the RMT modelling does not 'know' anything about the specific properties of the system under study. Since no physical parameters (except the global symmetries) are plugged in the RMT machinery, it is clear that its predictions are bounded by the existence of finite time scales. As far as transport properties are concerned, an important requirement for the validity of RMT is the ergodic time to be smaller than the average lifetime of a particle inside the chaotic cavity, in order for the particle to scatter off the chaotic boundary several times 'randomizing' its motion, before escaping through the leads.

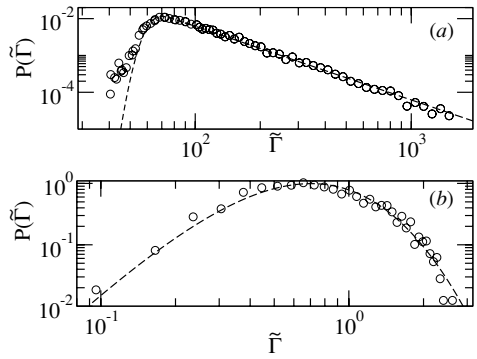

Figure 1. Distributions of the resonance widths in the ballistic regime for two different models: (*a*) the open kicked rotor [26] and (*b*) a fully connected quantum graph [6] with 'generic' vertex scattering matrices. The numerical data (○) are in excellent agreement with the RMT predictions of equation (9) (dashed lines).

In the general case, Fyodorov and Sommers [12] proved that the distribution of scaled resonance widths $\tilde{\Gamma} = \Gamma/\Delta$ for the unitary random matrix ensemble, is given by

$$\mathcal{P}(\tilde{\Gamma}) = \frac{(-1)^M}{\gamma(M)} \tilde{\Gamma}^{M-1} \frac{\mathrm{d}^M}{\mathrm{d}\tilde{\Gamma}^M} \left(\mathrm{e}^{-\tilde{\Gamma}\pi q} \frac{\sinh(\tilde{\Gamma}\pi)}{(\tilde{\Gamma}\pi)} \right), \qquad q = \frac{1 + |\langle S \rangle|^2}{1 - |\langle S \rangle|^2} \tag{9}$$

where the parameter q controls the degree of coupling with the channels, $\langle \cdots \rangle$ indicates an average over realizations and $\gamma(\cdot)$ is the γ-function. In figure 1 we report some representative results from two models in the ballistic regime together with the theoretical prediction (9). The excellent agreement is evident.

In the limit of $M \gg 1$, equation (9) reduces to the following expression [12]:

$$\mathcal{P}(\tilde{\Gamma}) = \begin{cases} \dfrac{M}{2\pi\tilde{\Gamma}^2}, & \text{for} \quad \dfrac{M}{\pi(q+1)} < \tilde{\Gamma} < \dfrac{M}{\pi(q-1)} \\ 0, & \text{otherwise} \end{cases} . \tag{10}$$

The following argument provides some intuition about the form of resonance width distribution (10). First we need to recall that the inverse of Γ represents the quantum lifetime of a particle in the corresponding resonant state escaping into the leads. Moreover, we assume that the particles are uniformly distributed inside the sample and spread ballistically until they reach the boundary, where they are absorbed. Then we can associate the corresponding lifetimes with the time $t_R \sim 1/\Gamma_R$ a particle needs to reach the boundaries, when starting a distance R away. This classical picture can be justified for all states with $\Gamma \gtrsim \Gamma_{\mathrm{cl}} \gg \Delta$ where Γ_{cl} is the classical decay rate which can be calculated numerically from the exponential decay of the classical probability to stay inside the sample. (For RMT models we have the so-called Moldauer–Simonius relation $\Gamma_{\mathrm{cl}} \sim \Delta M \ln(1 - |\langle S \rangle|^2)$ which gives us the lower bound in equation (10) while for generic chaotic system $\Gamma_{\mathrm{cl}} \sim \hbar(s/\Omega)v$ where s is the width of the opening, Ω is the total volume of the system and v is the velocity of the particle moving inside the system.) The relative number of states that require a time $t < t_R$ in order to reach the boundaries (or equivalently the number of states with $\Gamma > \Gamma_R$) of a d-dimensional system with linear dimension L, is

$$\mathcal{P}_{\mathrm{int}}(\Gamma_R) \equiv \int_{\Gamma_R}^{\infty} \mathcal{P}(\Gamma)\,\mathrm{d}\Gamma \sim \frac{V(t_R)}{L^d} = \frac{L^d - (L-R)^d}{L^d} \tag{11}$$

where $V(t_R) \sim L^d - (L-R)^d$ is the volume populated by all particles with lifetimes $t < t_R$. Assuming ballistic motion, i.e., $R = vt_R$, we get from equation (11) in the limit where $\Gamma \gg \Gamma_{\rm cl}$

$$\mathcal{P}_{\rm int}(\Gamma_R) \sim \frac{1}{\Gamma_R} \tag{12}$$

which eventually leads to the RMT prediction equation (10).

Equations (9) and (10) are our starting point. In the next subsections, we will investigate how deviations from these expressions arise as we increase the randomness of the system.

4.2. Diffusive regime

We start our presentation with the study of small resonance width distribution $\mathcal{P}(\Gamma < \Delta)$. The small resonances $\Gamma < \Delta$ can be associated with the existence of pre-localized states of the closed system (for a discussion on pre-localized states, see [21, 25–27]). They consist of a short-scale bump (where most of the norm is concentrated) and they decay rapidly in a power-law fashion from the centre of localization [21, 24, 26, 27]. One then expects that states of this type with localization centres at the bulk of the sample are affected very weakly by the opening of the system at the boundaries. In first order perturbation theory, considering the opening as a small perturbation we obtain [26, 62]

$$\frac{\Gamma}{2} = \langle \Psi | V^\dagger V | \Psi \rangle = \sum_{n \in \text{boundary}} |\Psi(n)|^2 \sim L^{d-1} |\Psi(L)|^2 \tag{13}$$

where $|\Psi(L)|^2$ is the wavefunction intensity of a pre-localized state at the boundary and d is the dimensionality of the sample. At the same time the distribution of wavefunction components at the boundary was found to be [24]

$$\mathcal{P}(\theta) \sim \exp\left(-A_\beta^{(d)} \ln^d(\theta^{4-d})\right), \qquad \theta = 1/L^{(d-1)/2}\Psi(L) \tag{14}$$

where the coefficient $A^{(d)} \propto \beta D$. Here $\beta = 1(2)$ denotes the corresponding ensemble for preserved (broken) time-reversal symmetry. Using equation (14) together with equation (13) we obtain

$$\mathcal{P}(\Gamma < \Delta) \sim \exp\left(-C_\beta^{(d)} \ln^d(1/\Gamma)\right) \qquad \text{where} \quad C_\beta \propto \beta D. \tag{15}$$

A detailed numerical analysis performed in [26, 62, 63] for the $d = 2, 3$ showed that the above perturbative derivation is valid as well for relatively large resonances, i.e., $\Delta < \Gamma < \Gamma_{\rm cl}$ where $\Gamma_{\rm cl} = D/L^2$ is the inverse Thouless time. In figure 2 we report some numerical data for the case $d = 2$ and compare with the theoretical predictions of equation (15). Let us finally compare equation (15) with the results for ballistic systems (see equation (10)). In the latter case a strip free of resonances is formed. In the diffusive regime, in contrast, there are pre-localized states, which are weakly coupled to the leads. Due to their existence the distribution of the small resonance widths has a non-trivial behaviour described by equation (15).

Next we turn to the analysis of $\mathcal{P}(\Gamma)$ for $\Gamma \gtrsim \Gamma_{\rm cl}$. Using the same argument that led to equation (11), but assuming now diffusive spreading, i.e., $R^2 = D \times t$, we get (to leading-order approximation with respect to $\Gamma_{\rm cl}/\Gamma$)

$$\mathcal{P}(\Gamma) \sim \left(\frac{1}{\Gamma}\right)^{\frac{3}{2}}, \tag{16}$$

valid for quasi one- [64], two- [25, 62] or three-dimensional [63] random media as long as the leads are attached to the boundary of the sample. We conclude that the different power-law

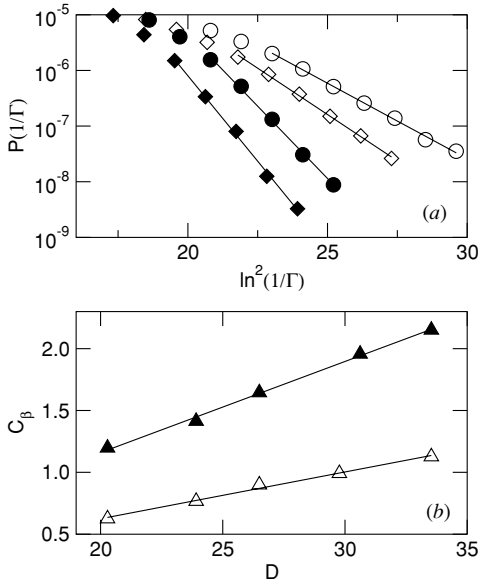

Figure 2. (*a*) The distribution of resonance widths (plotted as $\mathcal{P}(1/\Gamma)$ versus $1/\Gamma$) for $\Gamma < \Gamma_{\rm cl}$ for two representative values of D for the two-dimensional kicked rotator in the diffusive regime [26, 62]. The system size in all cases is $L = 80$. Full symbols correspond to broken TRS. The solid lines are the best fits of equation (15) for $\beta = 1(2)$ to the numerical data. (*b*) Coefficients C_β versus D for the same model as in (*a*) [26, 62]. The solid lines are the best fits to $C_\beta = A_\beta D + B_\beta$ for $\beta = 1(2)$. The ratio $R = A_2/A_1 = 1.95 \pm 0.03$.

decay of equation (16) with respect to equations (10) and (12) is a result of the different nature of the dynamics: ballistic versus diffusive.

Here it is interesting to point that a different way of opening the system might lead to a different power-law behaviour for $\mathcal{P}(\Gamma)$. Such a situation can be realized if instead of opening the system at the boundaries we introduce 'one-site' absorber (or one 'lead') somewhere inside the sample. In such a case for $d = 2$ we have

$$\mathcal{P}_{\rm int}(\Gamma_R) \sim \frac{V(t_R)}{L^2} = \frac{R^2}{L^2} = \frac{Dt_R}{L^2} \sim \frac{\Gamma_{\rm cl}}{\Gamma_R} \tag{17}$$

leading to the following power-law decay:

$$\mathcal{P}(\Gamma) \sim \left(\frac{1}{\Gamma}\right)^2. \tag{18}$$

Similarly, the analogue of equation (18) in $d = 3$ is

$$\mathcal{P}(\Gamma) \sim \left(\frac{1}{\Gamma}\right)^{2.5} \tag{19}$$

where we had to substitute $V(t_R) \sim R^3$. The above results are valid for any number M of 'leads' such that the ratio M/L^d scales as $1/L^d$.

If on the other hand we attach the open channel to the boundary (assume square geometry) of a 3D sample we come out with a decay law which is the same as that given by equation (18). This is due to the fact that the decay from the surface leads to a situation like that of a 2D system.

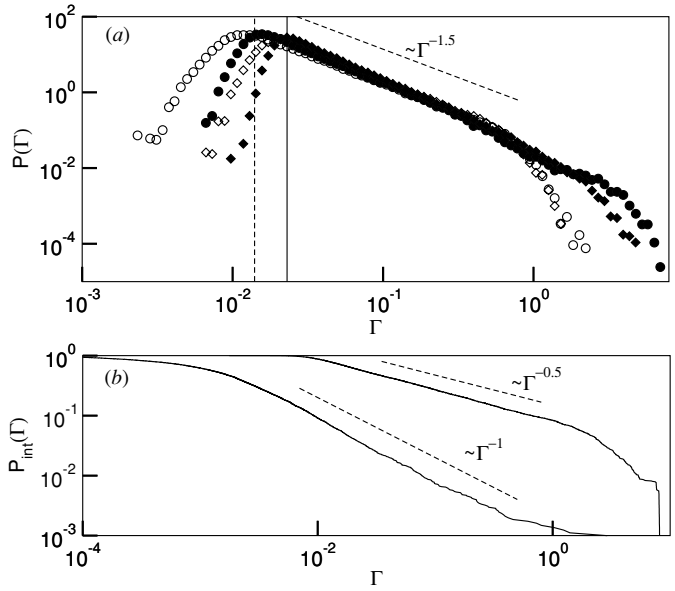

Figure 3. (*a*) The resonance width distribution $\mathcal{P}(\Gamma)$ for preserved TRS and $D = 20.3$ ($\circ$) and $D = 33.5$ ($\diamond$). The corresponding full symbols represent $\mathcal{P}(\Gamma)$ for broken TRS and the same values of D. The dashed (solid) vertical line marks the classical decay rate $\Gamma_{\rm cl}$ for $D = 20.3$ ($D = 33.5$). (*b*) The $\mathcal{P}_{\rm int}(\Gamma)$ for a sample with nine leads (the lower curve). For comparison, we also plot the $\mathcal{P}_{\rm int}(\Gamma)$ for the same sample but when we open the system from the boundaries. The dashed lines correspond to the theoretical predictions (16) and (18). The figure is taken from [62].

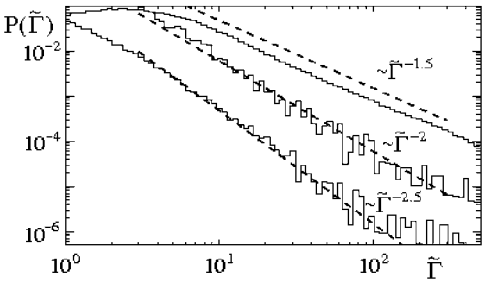

Figure 4. The resonance width distribution $\mathcal{P}(\tilde{\Gamma})$ for the 3D Anderson model [63] and various configurations of the open channels. The dashed lines are the corresponding theoretical predictions given by equations (16), (18) and (19) (see the text). The figure is taken from [63].

In figure 3 we present some numerical calculations of the 2D kicked rotator [62] while in figure 4 we present numerical data from the 3D Anderson model in the diffusive regime [63]. In all cases a comparison with the corresponding theoretical predictions (16), (18) and (19) shows a nice agreement.

4.3. Localized regime

Various groups [63, 65–67] have investigated the resonance width distribution in the localized regime during the past few years.

In the region of exponentially narrow resonances $\Gamma < \Gamma_0 = \exp(-2L/\xi)$ the distribution was found to be log-normal, i.e.,

$$\mathcal{P}(\tilde{\Gamma}) \sim \exp\left[-\left(4\frac{L}{\xi}\right)^{-1} \ln^2(\tilde{\Gamma})\right], \qquad \Gamma < \Gamma_0. \tag{20}$$

This is entirely analogous to the conductance distribution of localized systems. Equation (20) essentially relies on two assumptions: first that eigenfunction components are randomly distributed with no long-range correlations, and second that they are exponentially localized with a normal distribution of localization lengths. This part of the distribution becomes negligible at large L, because it comes of a fraction $\sim\xi/L$ of the full set of all resonances.

Instead, the long resonance tails behave as

$$\mathcal{P}(\tilde{\Gamma}) \sim \left(\frac{\xi}{L}\right)\frac{1}{\tilde{\Gamma}}, \qquad \Gamma_0 < \Gamma \ll 1/L. \tag{21}$$

Equation (21) can be easily understood once employing equation (11). The new ingredient now is that wavefunctions are exponentially localized, i.e., $|\Psi(r)| \sim (1/\xi^{d/2})\exp(-r/\xi)$. Using simple perturbation arguments, we have that (see equation (13)) $\Gamma \sim |\Psi(r)|^2$ which leads to the following approximation about the volume $V(t_R) \propto R^d \sim \xi^d \ln^d(\xi^d\Gamma)$. Inserting this in equation (11) we get (to leading-order approximation with respect to ξ/L) equation (21).

The large Γ region is essentially determined by the coupling to continuum, so it should be model dependent. Nevertheless, it is reasonable to assume that the number of resonances involved is constant, of order ξ, and therefore this extreme tail should subside at large L, at a rate $\sim\xi/L$.

From equations (20) and (21) it becomes evident that $\mathcal{P}(\tilde{\Gamma})$ depends on one parameter; namely, the dimensionless parameter ξ/L. This dimensionless parameter is the cornerstone of the 1-parameter scaling theory of localization [20]. It was shown in the past that the dimensionless conductance g is a simple function of ξ/L. The above theoretical considerations were tested [63, 66, 67] for various disordered and chaotic systems with dynamical localizations and were found to describe nicely the numerical data. In figure 5 we report some representative cases from the 3D Anderson model [63] in the localized regime.

Let us finally note that in the thermodynamic limit $L \to \infty$ the probability of finding an eigenstate at any finite distance from the boundary is equal to zero. Thus the distribution of the resonance widths in this case approaches a delta-function centred at zero.

4.4. Criticality

The statistical properties of various observables at the MIT are one of the most intriguing problems for many years now. Actually, despite the rich activity [18, 21, 24, 29, 35, 37, 39] very few theoretical results are known. Here, we present consequences of the MIT on the statistical properties of the rescaled resonance widths $\tilde{\Gamma}$. It was found [68] that $\mathcal{P}(\tilde{\Gamma})$ follow a new universal distribution, i.e., independent of the microscopic details of the random potential, and number of channels M as can be seen from figure 6. For small resonance widths, i.e., $\tilde{\Gamma} < 1$, it was found [63] that $\mathcal{P}(\tilde{\Gamma})$ can be fitted nicely with a log-normal. This behaviour resembles the one found for the small resonances in the localized regime (see equation (20)) although the character of wavefunctions here is much more complicated (multi-fractal versus exponentially localized states). The simplicity of the functional form is quite intriguing and a theoretical understanding is desirable. The sharp peak on the extreme right corresponding to very large resonances is non-universal (model specific) and statistically insignificant since it subsides as L increases like $M/L^3 \sim L^{-1}$ (see also discussion in the previous section).

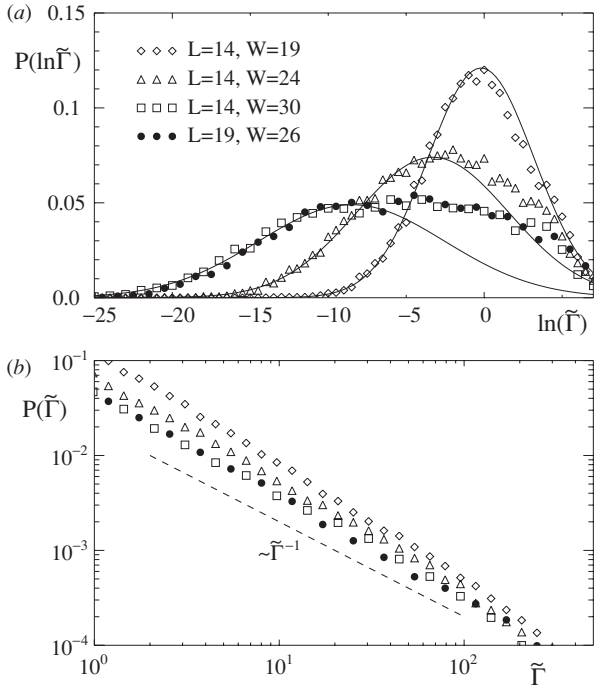

Figure 5. $\mathcal{P}(\tilde{\Gamma})$ in the localized regime for various combinations of W and L in the range $\tilde{\Gamma} \leqslant 1$. The log-normal decay is highlighted by Gaussian fits (full curves) whose maximum decreases with increasing strength of disorder and also shifts towards smaller values of $\tilde{\Gamma}$. Keeping the ratio $\xi/L \approx 0.136$ fixed, coinciding distributions (full circles and open squares) are obtained for different combinations of L, W. (*b*) For $\tilde{\Gamma} \geqslant 1$ the anticipated power-law decay $\mathcal{P}(\tilde{\Gamma}) \sim 1/\tilde{\Gamma}$ is observed (the dashed line) which becomes more robust for increasing strength of disorder. The figure is taken from [63].

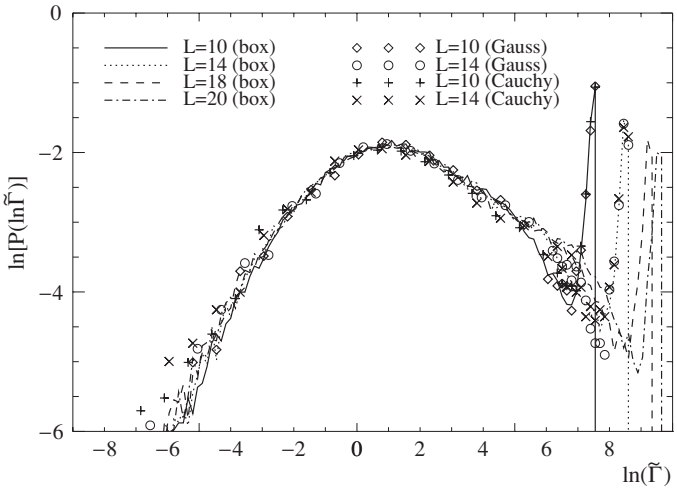

Figure 6. Universal behaviour of $\mathcal{P}(\tilde{\Gamma})$ at the MIT for a 3D Anderson model. The figure is taken from [68].

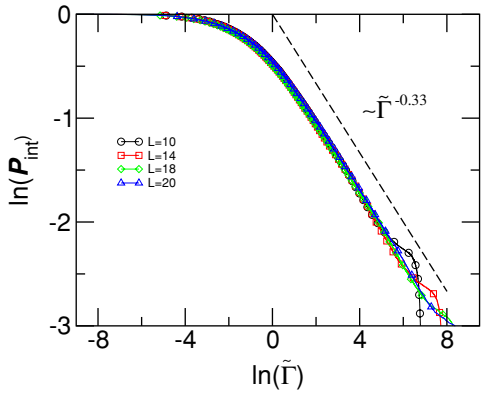

Figure 7. The integrated distribution $\mathcal{P}_{\rm int}(\tilde{\Gamma})$ for the 3D Anderson model at MIT [63, 68]. The dashed line is the theoretical prediction (22) corresponding to $\mathcal{P}_{\rm int}(\tilde{\Gamma}) \sim \tilde{\Gamma}^{-0.333}$ for our case. The figure is taken from [63, 68].

On the other hand, the main part of $\mathcal{P}(\tilde{\Gamma})$, corresponding to intermediate large resonances, follows a power-law which is different from that found for ballistic, diffusive or localized systems (see previous sections), i.e.,

$$\mathcal{P}(\tilde{\Gamma}) \sim g_{\rm c}^{1/d} \tilde{\Gamma}^{-(1+1/d)}. \tag{22}$$

where $g_{\rm c}$ is the Thouless conductance at criticality.

One can relate the power-law decay (22) to the anomalous diffusion at the MIT. Indeed, at MIT the conductance of a d-dimensional disordered sample has a finite value $g_{\rm c} \sim 1$. Approaching the MIT from the metallic side one has $g \sim E_T/\Delta$, where $E_T = D/R^2$ is the Thouless energy, D is the diffusion coefficient, and $\Delta \sim 1/R^d$ is the mean level spacing in a d-dimensional sample with linear size R. This yields $D \sim g_{\rm c}/R^{d-2}$ at critical disorder W_c. Taking into account that $D = R^2/t$, we get for the spreading of an excitation at the MIT

$$R^d(t) \sim g_{\rm c} t. \tag{23}$$

A straightforward application of equation (11) then leads to equation (22). In figure 7 we report some numerical results for the 3D Anderson model at MIT [63, 68]. An inverse power law $\mathcal{P}_{\rm int}(\tilde{\Gamma}) \sim \tilde{\Gamma}^{-\alpha}$ is evident. The best fit to the numerical data yields $\alpha = 0.333 \pm 0.005$ in accordance with equation (22).

In the original proposal of the scaling theory of localization, the conductance g is the relevant parameter [20]. A manifestation of this statement is seen in equation (22) where $\mathcal{P}^0_{\rm int} \equiv \mathcal{P}_{\rm int}(\tilde{\Gamma}_0)$ is proportional to the conductance g. It is therefore natural to expect that $\mathcal{P}^0_{\rm int}$ will follow a scaling behaviour for finite L (and for some $\tilde{\Gamma}_0 \sim 1$), which is similar to that obeyed by the conductance g. It was therefore postulated in [63, 68] the following scaling hypothesis,

$$\mathcal{P}^0_{\rm int}(W, L) = f(L/\xi(W)), \tag{24}$$

where $\xi(W)$ is the correlation length at MIT. In the insulating phase ($W > W_c$) the conductance of a sample with length L behaves as $g(L) \sim \exp(-L/\xi)$ due to the exponential localization of the eigenstates, and therefore we have $g(L_1) < g(L_2)$ for $L_1 > L_2$. Based on equation (22) we expect the same behaviour for $\mathcal{P}^0_{\rm int}$, i.e., for every finite $L_1 > L_2$ we must have $\mathcal{P}^0_{\rm int}(W, L_1) < \mathcal{P}^0_{\rm int}(W, L_2)$. On the other hand, in the metallic regime ($W < W_c$) we have that $g(L) = DL^{d-2}$ and therefore for $d > 2$, we expect from equation (22)

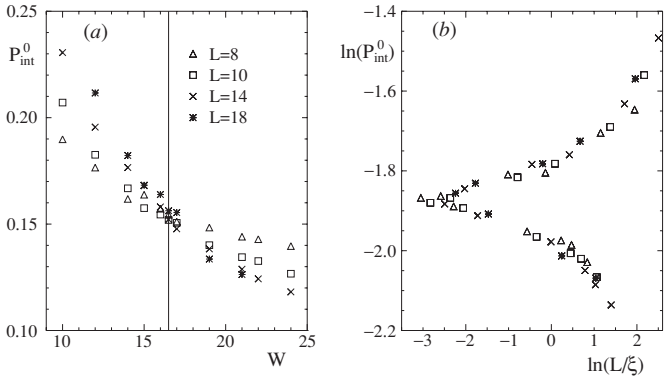

Figure 8. (*a*) $\mathcal{P}^0_{\rm int}(W, L)$ as a function of disorder strength W for different system sizes L provides a means to determine the critical point W_c of the MIT (the vertical line at $W_c = 16.5$). (*b*) The 1-parameter scaling of $\mathcal{P}^0_{\rm int}(W, L)$ (equation (24)) is confirmed for various system sizes L and disorder strengths W using the box distribution. The figure is taken from [63, 68].

$\mathcal{P}^0_{\rm int}(W, L_1) > \mathcal{P}^0_{\rm int}(W, L_2)$. Thus, the critical point is that at which the size effect changes its sign, or in other words, the point where all curves $\mathcal{P}^0_{\rm int}(W, L)$ for various L cross. One can reformulate the last statement by stating that in the thermodynamic limit $L \to \infty$ at $W = W_c$ the number of resonances with width larger than the mean level spacing goes to a constant.

In figure 8(*a*), we show the evolution of $\mathcal{P}^0_{\rm int}(W)$ for different L using the box distribution [63, 68]. From this analysis the critical disordered strength $W = W_c = 16.5 \pm 0.5$ was determined in [63, 68] in agreement with other calculations [18, 40]. A further verification of the scaling hypothesis (24) is shown in figure 8(*b*) where the same data are reported as a function of the scaling ratio L/ξ. All points collapse on two separate branches for $W < W_c$ and $W > W_c$.

5. Delay times

We turn now to the analysis of Wigner and proper delay times as defined in equation (4) above. Their knowledge is relevant for experiments on frequency and parameter-dependent transmission through chaotic microwave cavities [8, 32] or semiconductor quantum dots with ballistic point contacts [69]. Also, it can be shown that they are related to the distribution of reflection coefficients R in the presence of weak absorption.

Absorption is one of the main ingredients in actual experimental situations and has gained much interest in the past few years (see [43] and [13] in this volume). Unfortunately, a comprehensive treatment of absorption is still lacking. There are only very few reported analytical results for the distribution $\mathcal{P}(R)$ of the reflection coefficient $R = S^\dagger S$ in the presence of absorption and all of them are within the regime of applicability of RMT [43, 70, 71], except the recent work [72, 73], where quasi-1D geometry in the localized regime is considered as well.

Specifically, in the weak absorption limit it was shown [8, 70] that the following relation holds,

$$R_q = 1 - \tau_q/\tau_a, \tag{25}$$

where τ_q are the proper delay times (eigenvalues of the Wigner–Smith operator) and $1/\tau_a$ is the absorption rate. Thus the knowledge of $\mathcal{P}(R)$ reduces to the calculation of the distribution of proper delay times $\mathcal{P}(\tau_q)$ [70].

For one channel the distribution of delay times is now quite well understood and studied in all regimes. Quite recently [74] the existence of a very general relation between the delay time distribution and the distribution of eigenfunction intensities was shown,

$$\left\langle \tilde{\tau}_W^{-k} \right\rangle = \langle y^{k+1} \rangle, \tag{26}$$

where $y = \Omega|\psi_n(r)|^2$ is the local eigenfunction intensity and $\tilde{\tau}_W = \tau_W \Delta/2\pi$. Equation (26) leads to the following functional relation between the two distributions:

$$\tilde{\mathcal{P}}_W(\tilde{\tau}_W) = \frac{1}{\tilde{\tau}_W^3} \mathcal{P}_y\left(\frac{1}{\tilde{\tau}_W}\right). \tag{27}$$

On the one hand, this relation allows us to use the existent knowledge on eigenfunction statistics [21] to provide explicit expressions for delay times distributions in various regimes of interest. On the other hand, since phase shifts and delay times are experimentally measurable quantities, especially in the one-channel reflection experiment [8, 70, 75–77], this relation opens a new possibility for experimental study of eigenfunctions.

5.1. Ballistic regime

We start again our presentation from the ballistic regime. The notion of proper delay times goes back more than 40 years to the seminar paper of Smith [44]. Although many authors have worked on this problem [12, 78–82], only recently its probability distribution was calculated. It was shown in [83], using standard RMT methods, that the distribution of inverse proper delay times is given by the Laguerre ensemble from random matrix theory

$$\mathcal{P}\left(\tau_1^{-1}, \ldots, \tau_M^{-1}\right) \propto \prod_{i<j} \left|\tau_i^{-1} - \tau_j^{-1}\right|^{\beta} \prod_k \left|\left(\tau_i^{-1}\right)^{\beta M/2} \exp^{-\beta 2\pi\hbar\tau_k^{-1}/2\Delta}\right. . \tag{28}$$

As a matter of fact from equation (28) one can evaluate the distribution of Wigner delay times τ_W, which for large values decays as a power law

$$\mathcal{P}(\tau_W) \propto \frac{1}{\tau_W^{2+\beta M/2}} \tag{29}$$

in agreement with an earlier conjecture by Fyodorov and Sommers [12].

Specifically for $M = 1$ the distribution of Wigner delay times was calculated even in the crossover regime between unitary ($\beta = 2$) and orthogonal ($\beta = 1$) symmetry classes and was found to be [84]

$$\mathcal{P}_W(\tilde{\tau}_W) = \frac{1}{2\tilde{\tau}_w^3} \int_{-1}^{1} \mathrm{d}\lambda \int_1^{\infty} \mathrm{d}\lambda_2\, \lambda_2^2\, \mathrm{e}^{-X^2(\lambda_2^2-1)}\, \mathrm{e}^{-\lambda_2^2/\tilde{\tau}_W} I_0\left[\frac{\lambda_2\sqrt{\lambda_2^2-1}}{\tilde{\tau}_W}\right] \mathcal{I}_2(\lambda, \lambda_2), \tag{30}$$

$$\mathcal{I}_2(\lambda, \lambda_2) = 2X^2\left[(1-\lambda^2)\,\mathrm{e}^{-\alpha} + \lambda_2^2(1-\mathrm{e}^{-\alpha})\right] - (1-\mathrm{e}^{-\alpha}), \tag{31}$$

where $\alpha = X^2(1-\lambda^2)$, $I_0(z)$ stands for the modified Bessel function, and X is a crossover driving parameter. For pure symmetries, equation (30) leads to [12, 74, 78]

$$\mathcal{P}(\tilde{\tau}_W) = [(\beta/2)^{\beta/2}/\gamma(\beta/2)]\tilde{\tau}_W^{-\beta/2-2} \exp^{-\beta/2\tilde{\tau}_W}. \tag{32}$$

The following simple argument can be used in order to understand the tails of the Wigner delay time distribution equation (29). Our starting point is the well-known relation

$$\tau_W(E) = \sum_{n=1}^{M} \frac{\Gamma_n}{(E-E_n)^2 + \Gamma_n^2/4} \tag{33}$$

which connects the Wigner delay times and the poles of the S-matrix.

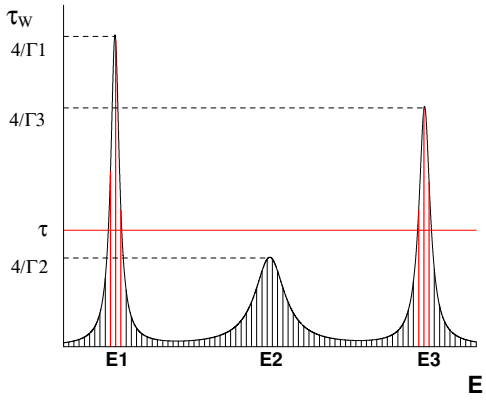

Figure 9. Schematic plot for the Wigner delay time as a function of energy according to equation (33).

It is evident that large times $\tau_W(E) \sim \Gamma_n^{-1}$ correspond to the cases when $E \simeq E_n$ and $\Gamma_n \ll 1$. In the neighbourhood of these points, $\tau(E)$ can be approximated by a single Lorentzian (33). Sampling the energies E with step $\Delta E \ll \Gamma_{\min}$ we calculate the number of points for which the time delay is larger than some fixed value τ (see figure 9). Assuming that the contribution of each Lorentzian is proportional to its width one can estimate this number as $\sum_{\Gamma_n<1/\tau} \Gamma_n/\Delta E$. For the integrated distribution of delay times in the limit $\Delta E \to 0$ we obtain

$$\mathcal{P}_{\rm int}(\tau_W) \sim \int^{1/\tau_W} {\rm d}\Gamma\, \mathcal{P}(\Gamma)\Gamma \tag{34}$$

and by substituting the small resonance width asymptotic given by equation (9) we come out with the power-law expression (29).

5.2. *Diffusive regime*

Using the general relation (27) for the case of $M = 1$, we find for $\mathcal{P}(\tau_W)$ [74]

$$\begin{aligned}
\mathcal{P}_w(\tilde\tau_W) &= \frac{{\rm e}^{-1/2\tilde\tau_W}}{\sqrt{2\pi}\,\tilde\tau_W^{5/2}}\left[1+\frac{\kappa}{2}\left(\frac{3}{2}-\frac{3}{\tilde\tau_W}+\frac{1}{2\tilde\tau_W^2}\right)+\cdots\right] && \beta = 1,\\
\mathcal{P}_w(\tilde\tau_W) &= \frac{{\rm e}^{-1/\tilde\tau_W}}{\tilde\tau_W^3}\left[1+\frac{\kappa}{2}\left(2-\frac{4}{\tilde\tau_W}+\frac{1}{\tilde\tau_W^2}\right)+\cdots\right] && \beta = 2,\\
\mathcal{P}_w(\tilde\tau_W) &= \frac{4\,{\rm e}^{-2/\tilde\tau_W}}{\tilde\tau_W^4}\left[1+\frac{\kappa}{2}\left(3-\frac{6}{\tilde\tau_W}+\frac{2}{\tilde\tau_W^2}\right)+\cdots\right] && \beta = 4,
\end{aligned} \tag{35}$$

where the parameter $\kappa \propto g^{-1}$ is inversely proportional to the dimensionless conductance g. The proportionality coefficient depends essentially on the sample geometry and on the coordinates of the lead. Note that in the limit of $g \to \infty$ we recover the RMT results discussed in the previous section.

Equation (35) holds for relatively large delay times $\tilde\tau_W \gtrsim \sqrt{\kappa}$, while in the opposite case the distribution is dominated by the existence of the anomalously localized states and has the

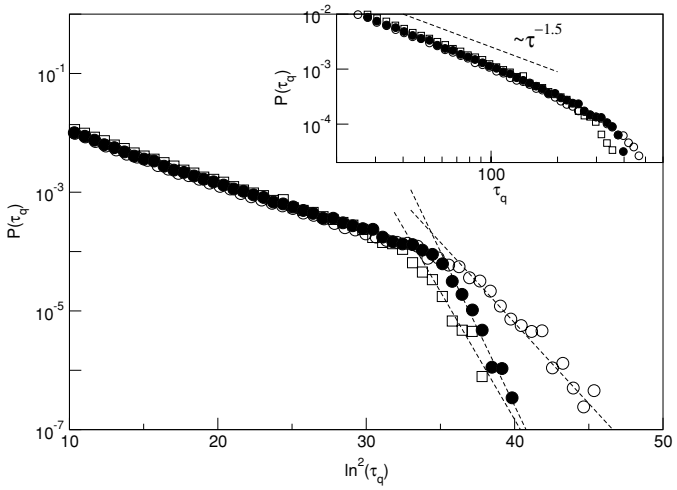

Figure 10. The proper delay times distribution $\mathcal{P}(\tau_q)$ for a 2D kicked rotator [26] with diffusive coefficients $D = 20.3$ (○) and $D = 29.8$ (□). The '•' corresponds to $D = 20.3$ but now with broken TRS. The dashed lines have slopes equal to C_β extracted from the corresponding $\mathcal{P}(\Gamma)$ (see figure 8). In the inset, we report $\mathcal{P}(\tau_q)$ for moderate values of τ_q in a double logarithmic scale. The figure is taken from [26, 62].

following behaviour for dimensionality $d = 2, 3$ [74]:

$$\mathcal{P}_W(\tilde{\tau}_W) \sim \exp\left(\frac{\beta}{2}\left\{-\frac{1}{\tilde{\tau}_W} + \kappa\frac{1}{\tilde{\tau}_W^2} + \cdots\right\}\right), \qquad \kappa \lesssim \tilde{\tau}_W \lesssim \sqrt{\kappa}, \tag{36}$$

$$\mathcal{P}_W(\tilde{\tau}_W) \sim \exp(-C_d \ln^d(1/\tilde{\tau}_W)), \qquad \tilde{\tau}_W \lesssim \kappa. \tag{37}$$

The coefficient C_d depends not only on the dimensionality of the system, but on the symmetry parameter β as well (for a discussion on these issues, see [24, 26, 74] and references therein).

For many open channels $M \gg 1$ there are no quantitative theoretical results yet. However, one can employ qualitative arguments which together with numerical findings can allow us to understand the resulting distributions. Indeed, substituting in equation (34) the small resonance width asymptotic for the $\mathcal{P}(\Gamma)$ given by equation (15) we come out with the following log-normal law for the large τ regime

$$\mathcal{P}\left(\tau_W > \Gamma_{\rm cl}^{-1}\right) \sim \exp(-C_\beta \ln^d \tau) \tag{38}$$

where the coefficient C_β is the same as the one given in equation (15). This prediction has been tested numerically in [25, 26] for the case of a 2D diffusive system, and the numerical findings (see figure 10) were shown to be in excellent agreement.

Now we estimate the behaviour of $\mathcal{P}(\tau_W)$ for $\tau_W \lesssim \Gamma_{\rm cl}^{-1}$. In this regime many short-living resonances contribute to the sum (33). We may therefore consider τ as a sum of many independent positive random variables each of the type $\tau_n = \Gamma_n x_n$, where $x_n = \delta E_n^{-2}$. Assuming further that δE_n are uniformly distributed random numbers we find that the distribution $\mathcal{P}(x_n)$ has the asymptotic power-law behaviour $1/x_n^{3/2}$. As a next step we find that the distribution $\mathcal{P}(\tau_n)$ decays asymptotically as $1/\tau_n^{3/2}$ where we use that $\mathcal{P}(\Gamma_n) \sim 1/\Gamma_n^{3/2}$. Then the corresponding $\mathcal{P}(\tau)$ is known to be a stable asymmetric Levy distribution $L_{\mu,1}(\tau)$ of index $\mu = 1/2$ [85] which has the following form at the origin,

$$\mathcal{P}\left(\tau \lesssim \Gamma_{\rm cl}^{-1}\right) \sim \frac{1}{\tau^{3/2}} \exp(-\sigma/\tau_W), \tag{39}$$

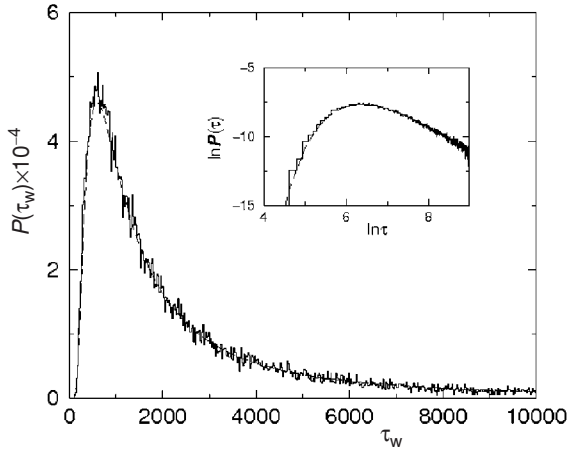

Figure 11. Distribution of the delay times $\mathcal{P}(\tau_W)$ for the 1D Anderson model with on-site potential, uniformly distributed between $[-0.1; 0.1]$ and wavenumber $k = \sqrt{\pi}$. The dashed line corresponds to (40). In the inset, we present the same data in a log–log plot. The figure is taken from [87].

where σ is some constant of order unity. Simple theoretical arguments [12] suggest that this part of the distribution of the Wigner delay times is the same as in RMT considerations. This is in contrast with the large delay times (see equation (38)) where RMT considerations lead to a power-law decay (29).

Since $\tau_W = \sum_{i=1}^{M} \tau_q$, we expect the behaviour of the distribution of proper delay times $\mathcal{P}(\tau_q)$ to be similar to $\mathcal{P}(\tau)$ for large values of the arguments (for $\tau \gg 1$ we have $\tau \sim \tau_q^{\max}$). The above predictions were verified numerically for a 2D diffusive system [26], while unpublished results [63] show that the same law applies for a 3D diffusive system as well. We point out here that the asymptotic behaviour $\mathcal{P}(\tau) \sim 1/\tau^{3/2}$ emerges also for chaotic/ballistic systems where the assumption of uniformly distributed δE_n is the only crucial ingredient (see, for example, [12]).

5.3. Localized regime

In a series of recent works [86–89] it was found that for 1D systems with $M = 1$ and weak disorder the delay time distribution is (see figure 11)

$$\mathcal{P}(\tau_W) = \frac{\xi}{v\tau_W^2} \exp(-\xi/v\tau_W), \tag{40}$$

where ξ is the localization length and $v = |\partial E/\partial k|$ is the group velocity. Equation (40) takes its maximum value at $\tau_W^{\max} = 0.5\xi/v$, indicating that the most probable trajectory that a particle travels (forth and back) before it scatters outside the sample is the mean free path $l_{\text{mean}} = \xi/4$. As $\tau_W \to \infty$, $\mathcal{P}(\tau_W)$ shows a long time tail which goes as $2\tau_W^{\max}/\tau_W^2$. This leads to a logarithmic divergence of the average value of τ_W, indicating the possibility of the particle traversing the infinite sample before being totally reflected. As was indicated in [87–89] this is another manifestation of the fact that in the localized regime the conductance shows log-normal distribution due to the presence of Azbel resonances.

We note that although the distribution for small delay times depends on disorder strength and possibly on the number of channels M, the long time tail is universal. As a matter of fact one can understand the long time power-law behaviour by employing the argument leading to

equation (34). Indeed by substituting the resonance distribution in the localized regime (21) we get again $\mathcal{P}(\tau_W) \propto 1/\tau_W^2$ independent of the number of channels M. The validity of this calculation was checked recently [63] for the 3D Anderson model in the localized regime and for $M \gg 1$ channels.

The above expression (40) does not contain the length of the chain, indicating that this intermediate asymptotics of the delay time distribution is related to the resonance width distribution, which is dominated by the electron escape rate from the resonant state into the nearest reservoir and for $L \to \infty$ is exact for any delay time. However, the finite length L determines a cutoff $\tau_W \sim e^{L/\xi}$ for this universal behaviour, and for larger delay times we find [88]

$$\mathcal{P}(\tau_W) \propto \exp(-L/\xi)\tau_W^{-(1+\frac{\xi}{L}\ln\tau_W)}, \qquad \tau_W > e^{L/\xi}. \tag{41}$$

We mark that equation (41) was recently derived in [72] for the case of quasi-1D random systems.

5.4. Criticality

Recently, an intensive activity to understand $\mathcal{P}(\tau_W)$ for systems at critical conditions was undertaken in [68, 72, 74, 90]. The activity was mainly concentrated in the simplest scattering set-up of one open channel attached to the system of linear size L. As a result, an anomalous scaling of inverse moments of τ_W with the system size L was reported [74, 90] and specific predictions linking the scaling exponents and the multi-fractal properties of eigenfunctions of the corresponding closed system were made. Specifically, it was found that the inverse moments of Wigner delay times $\langle \tau_W^{-q} \rangle$ scale as

$$\langle \tau_W^{-q} \rangle \propto L^{-f(q)}, \qquad f(q) = q D_{q+1} \tag{42}$$

where $\langle \cdot \rangle$ stands for an ensemble average. However, it was found that this relation is extremely fragile [90]; namely, it holds for channels attached to a *typical* position inside the sample. This excludes the standard scattering set-up where the channel is attached to the edge of the sample.

In figure 12 we summarize the results of the investigation undertaken in [90] where the analysis was performed for the power banded random matrix (PBRM) model, whose elements are independent random variables H_{ij} with the variance decreasing in a power-law fashion: $\langle (H_{ij})^2 \rangle = [1 + (|i-j|/b)^{2\alpha}]^{-1}$. For $\alpha = 1$ this model shows critical behaviour and the fractal dimensions D_q of the eigenfunctions depend on the parameter b and can be calculated analytically [21, 91]. In figure 12(*a*) we report the results for the case with a channel attached to the boundary. We see that the numerical data deviate from the theoretical predictions for any value of b. Instead, the agreement is very good for the case where the channel is attached to the bulk of the sample (see figure 12(*b*)). In the latter case, the channel is attached to a *representative* position in the sample. These results will provide a new method for evaluating the fractal dimensions D_q in microwave and light wave experiments where τ_W can be extracted even in the presence of weak absorption. At the same time the appearance of the anomalous scaling of $\langle \tau_W^{-q} \rangle$ can be used as a criterion for detecting MIT.

6. Quasi-periodic systems at criticality

Periodic and random media cover only the two extremes of the rich spectrum of complex systems. Quasi-periodic systems [92–100] form an intermediate regime and have fascinating properties. In these deterministic non-periodic structures translational order is absent. In their

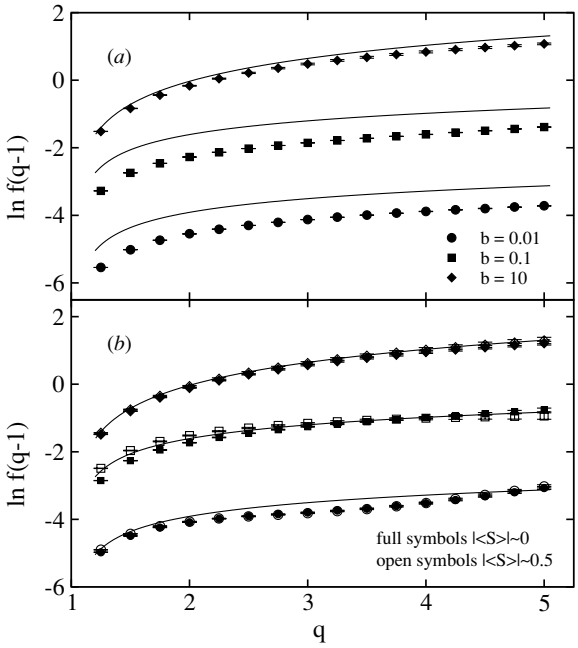

Figure 12. Scaling properties of inverse moments of delay times for the PBRM at criticality [90]. We report $\ln f(q-1)$ as a function of q for a channel attached (a) to the boundary and (b) to the bulk of the sample when $|\langle S\rangle| \sim 0$ (full symbols). In (b) we also show $\ln f(q-1)$ for $|\langle S\rangle| \sim 0.5$ (open symbols). The curves are the theoretical predictions of equation (42). The figure is taken from [90].

one-dimensional tight-binding formulation they are described mathematically by the following Hamiltonian,

$$\psi_{n+1} + \psi_{n-1} + W_n \psi_n = E\psi_n, \tag{43}$$

where W_n is given by some quasi-periodic sequence. Among the most well-studied representatives of this class are the Harper model [92, 97–99] and Fibonacci quasi-crystals [93–97, 99, 100]. These two systems have been the subject of an extensive theoretical and experimental effort in the last 20 years.

The Harper model is described by the tight-binding Hamiltonian (43) with the on-site potential given by $W_n = \lambda \cos(2\pi\phi n)$. This system effectively describes a particle in a two-dimensional periodic potential in a uniform magnetic field with $\phi = a^2 eB/hc$ being the number of flux quanta in a unit cell of area a^2. When ϕ is an irrational number, the period of the effective potential W_n is incommensurate with the lattice period. The states of the corresponding closed system are extended when $\lambda < 2$, and the spectrum consists of bands (the ballistic regime). For $\lambda > 2$ the spectrum is point-like and all states are exponentially localized (the localized regime). The most interesting case corresponds to $\lambda = 2$ of the MIT. At this point, the spectrum is a Cantor set with fractal (box counting) dimension $D_0^E \leqslant 0.5$ [92, 97, 99]. The spectral properties of the Harper model were recently investigated in microwave experiments [98]. Similar theoretical attention was also given to the study of eigenfunctions [92, 97] which show self-similar fluctuations on all scales.

The Fibonacci binary quasi-crystal attracted much interest as well. Here the potential W_n only takes the two values $+W$ and $-W$ arranged in a Fibonacci sequence [93]. It was shown [93, 95, 96] that the spectrum is a Cantor set with zero Lebesgue measure for all $W > 0$.

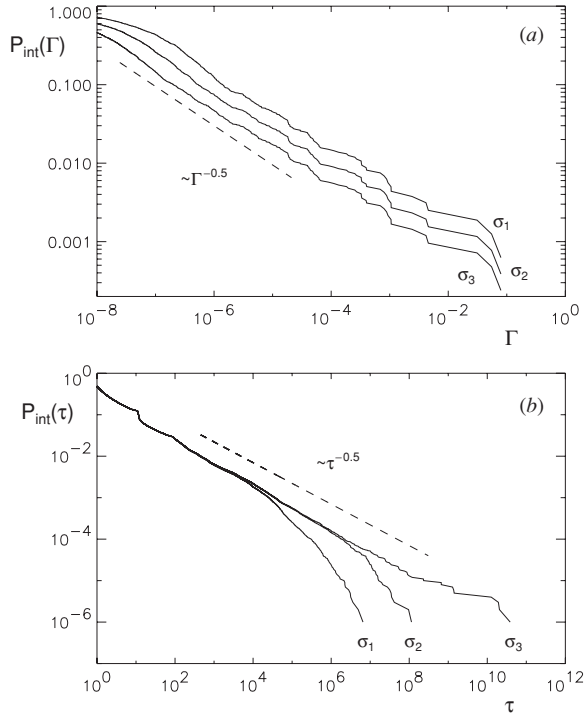

Figure 13. (*a*) $\mathcal{P}_{\rm int}(\Gamma)$ of the Harper model ($\lambda = 2$) for three approximants of σ_G, $\sigma_1 = \frac{987}{1597}$; $\sigma_2 = \frac{1597}{2584}$; $\sigma_3 = \frac{2584}{4181}$. An inverse power law $P_{\rm int}(\Gamma) \sim \Gamma^{1-\alpha}$ is evident. A least-squares fit yields $\alpha \approx 1.5$ in accordance with $D_0^E \simeq 0.5$ and equation (44). As is seen the lower cutoff of the scaling region decreases for higher approximants. (*b*) $\mathcal{P}_{\rm int}(\tau)$ of the Harper model ($\lambda = 2$) for three approximants of the golden mean $\sigma_1 = \frac{233}{377}$; $\sigma_2 = \frac{987}{1597}$; and $\sigma_3 = \frac{832\,040}{1\,346\,269}$. An inverse power law $P_{\rm int}(\tau) \sim \tau^{1-\gamma}$ is evident. A least-squares fit yields $\gamma \approx 1.5$ in accordance with $D_0^E \simeq 0.5$ and equation (44). As is seen, the upper cutoff of the scaling region increases for higher approximants. The figure is taken from [99].

The first experimental realization of Fibonacci super-lattices was reported in [94] while their optical analogues were realized in [96, 100].

In [99] we presented consequences of the fractal nature of the spectrum in open quasi-periodic systems. We considered open systems with one channel (the simplest possible scattering problem) and reported the appearance of a new type of resonance width and delay time statistics. These distributions show inverse power-law behaviour dictated by the fractal dimension D_0^E of the spectrum. Specifically, it was found that the probability distributions of resonance widths $\mathcal{P}(\Gamma)$ and of delay times $\mathcal{P}(\tau)$ when generated over *different energies*[1], behave as

$$\begin{aligned} \mathcal{P}(\Gamma) &= \Gamma^{-\alpha} \qquad & \alpha &= 1 + D_0^E \\ \mathcal{P}(\tau_W) &= \tau_W^{-\gamma} \qquad & \gamma &= 2 - D_0^E . \end{aligned} \tag{44}$$

Note that for $D_0^E = 0$ we recover the results (21) and (40) of the point-like spectrum $\left(D_0^E = 0\right)$ corresponding to a localized system.

[1] We note that distributions generated over different energies wash out multi-fractal wavefunction properties of a *specific* eigenstate as opposed to the calculation of section 5.4.

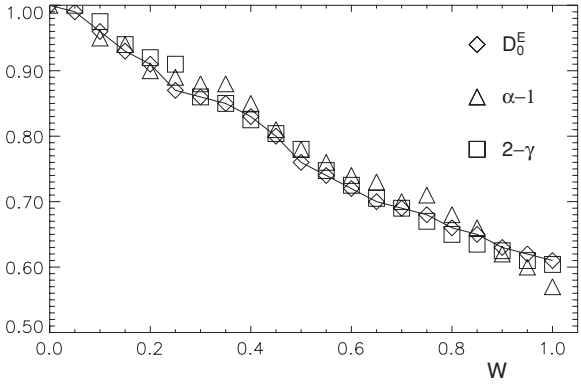

Figure 14. Power-law exponents α, γ (plotted as $\alpha - 1$ and $2 - \gamma$) of the resonance widths and of the delay time distributions, respectively, as a function of the potential strength W for the Fibonacci model. We also plot the fractal dimension D_0^E of the spectrum (the solid line is to guide the eye). Our numerical data show that α and γ are related to the Hausdorff dimension D_0^E according to equation (44). The figure is taken from [99].

The connection between the exponents α, γ and the fractal dimension D_0^E of the closed system calls for an argument for its explanation. The following heuristic argument [87], similar in spirit to that used in section 4.1, provides some understanding of the power laws (44). We consider successive rational approximants $\phi_i = p_i/q_i$ of the continued fraction expansion of ϕ. On a length scale q_i the periodicity of the potential is not manifest and we may assume that the variance of a wave packet spreads as $var(t) \sim t^{2D_0^E}$ [97]. We attach the lead at the end of the segment q_i which results in broadening the energy levels by a width Γ. The maximum time needed for a particle to recognize the existence of the leads is $\tau_{q_i} \sim q_i^{1/D_0^E}$. The latter is related to the minimum level width $\Gamma_{q_i} \sim 1/\tau_{q_i}$. The number of states living in the interval is $\sim q_i$ and thus determines the number of states with resonance widths $\Gamma > 1/\tau_{q_i}$. Thus $\mathcal{P}_{\rm int}(\Gamma_{q_i}) \sim q_i \sim \Gamma^{-D_0^E}$. By repeating the same argument for higher approximants $\phi_{i+1} = p_{i+1}/q_{i+1}$ we conclude that $\mathcal{P}(\Gamma) \sim \Gamma^{-(1+D_0^E)}$, in agreement with (44). Furthermore, use of equation (34) of section 5.1 results in the distribution (44) for the Wigner delay times. The numerical results (see figures 13 and 14) obtained for the Harper and the Fibonacci models in [87] verify the validity of the above arguments. Nevertheless, a rigorous mathematical proof is still lacking.

7. Conclusions

In this paper, we summarized the recent activity on the statistical properties of resonances and delay times of random/chaotic systems and analysed the deviations from the universal RMT predictions due to effects related to Anderson localization, diffusion and criticality. We have found that the tails of the resonance width distribution $\mathcal{P}(\Gamma)$ reflect the nature of the *dynamics* associated with the corresponding closed system as it is defined by the second moment of a spreading wave packet (ballistic, diffusive, critical, or localized). Instead, the origin, corresponding to small resonance widths, is dictated by anomalously localized states. Moreover, we have found that in the diffusive regime $\mathcal{P}(\Gamma)$ is affected by the channel 'configuration' (position and relative number) as well, in contrast to the localized regime. At MIT the resonance width distribution is universal and can be used to formulate a scaling theory of localization.

Localization phenomena affect also the delay times leaving their traces to the distributions $\mathcal{P}(\tau)$. For scattering systems attached to one open channel, we have a very good quantitative understanding of $\mathcal{P}(\tau)$ for all regimes. A general expression connects this distribution with the distribution of wavefunction intensities, the latter being well studied during the past few years. This connection allows us to use the experimentally accessible delay times in order to probe properties of wavefunctions, like multi-fractality, which are not easily measured. For many open channels, ample numerical data supported by theoretical arguments allow us to estimate the shape of the distribution of delay times and get a qualitative understanding of the traces of localization. Nevertheless, it remains a challenge to get some quantitative expressions as well.

The last section of this paper is devoted to the 1D quasi-periodic systems at criticality. The corresponding closed systems show fascinating properties like spectral and wavefunctions fractality. We reviewed the traces of spectral fractality to the distributions of the resonance widths $\mathcal{P}(\Gamma)$, and of delay times $\mathcal{P}(\tau)$. Based on numerical results and theoretical arguments, it is shown that both quantities decay algebraically with powers which are related to the fractal (box counting) dimension D_0^E of the spectrum of the closed system.

Acknowledgments

We acknowledge many useful discussions with Y Fyodorov, T Geisel, A Mendez-Bermudez, A Ossipov, D Savin, H Schanz, B Shapiro, U Smilansky and M Weiss. This work was supported by a grant from the GIF, the German-Israeli Foundation for Scientific Research and Development.

References

[1] Mahaux C and Weidenmüller H A 1969 *Shell Model Approach in Nuclear Reactions* (Amsterdam: North-Holland)
Rotter I 1991 *Rep. Prog. Phys.* **54** 635
Verbaarschot J J M, Weidenmüller H A and Zirnbauer M R 1985 *Phys. Rep.* **129** 367
[2] Nayfeh M H *et al* (ed) 1989 *Atomic Spectra and Collisions in External Fields* vol 2 (New York: Plenum)
[3] Gaspard P 1991 *'Quantum Chaos', Proc. E Fermi Summer School* ed G Casati *et al* (Amsterdam: North-Holland) p 307
[4] Beenakker C 1997 *Rev. Mod. Phys.* **69** 731
[5] Smilansky U 1989 *Les Houches Summer School on Chaos and Quantum Physics* ed M-J Giannoni *et al* (Amsterdam: North-Holland) pp 371–441
[6] Kottos T and Smilansky U 2000 *Phys. Rev. Lett.* **85** 968
Kottos T and Smilansky U 2003 *J. Phys. A: Math. Gen.* **36** 3501
[7] Stöckmann H-J 1999 *Quantum Chaos: An Introduction* (Cambridge: Cambridge University Press)
Kogan E, Mello P A and Liqun H 2000 *Phys. Rev.* E **61** R17
Beenakker C W J and Brouwer P W 2001 *Physica* E **9** 463
[8] Doron E, Smilansky U and Frenkel A 1990 *Phys. Rev. Lett.* **65** 3072
Stöckmann H J and Stein J 1990 *Phys. Rev. Lett.* **64** 2215
Stein J, Stöckmann H-J and Stoffregen U 1995 *Phys. Rev. Lett.* **75** 53
[9] Nockel J U and Stone A D 1997 *Nature* **385** 45
Gmachl C *et al* 1998 *Science* **280** 1556
[10] Wiersma D S, Van Albada M P and Lagendijk A 1995 *Nature* **373** 203
Genack A Z *et al* 1999 *Phys. Rev. Lett.* **82** 715
[11] Raizen M, Salomon C and Niu Q 1997 *Phys. Today* **50** 30–4
[12] Fyodorov Y V and Sommers H-J 1997 *J. Math. Phys.* **38** 1918
Fyodorov Y V and Khoruzhenko B A 1999 *Phys. Rev. Lett.* **83** 65
Sommers H J, Fyodorov Y V and Titov M 1999 *J. Phys. A: Math. Gen.* **32** L77

[13] Kuhl U, Stöckmann H-J and Weaver R 2005 *J. Phys. A: Math. Gen.* **38** 10433–63
[14] Genack A and Chabanov A A 2005 *J. Phys. A: Math. Gen.* **38** 10465–88
[15] Hemmady S, Zheng X, Antonsen Th M Jr, Ott E and Anlage S M 2005 *Proc. 2nd Workshop on Quantum Chaos and Localisation Phenomenon (Poland: Warsaw), Acta Phys. Pol. A* to be published (*Preprint* nlin.CD/0506025)
Hemmady S, Zheng X, Ott E, Antonsen Th M and Anlage S M 2005 *Phys. Rev. Lett.* **94** 014102
[16] Altshuler B L, Kravtsov V E and Lerner I V 1991 *Mesoscopic Phenomena in Solids* ed B L Altshuler, P A Lee and R A Webb (Amsterdam: North-Holland)
[17] Izrailev F M 1990 *Phys. Rep.* **196** 299
Fishman S, Grempel D R and Prange R E 1982 *Phys. Rev. Lett.* **49** 509
[18] Anderson P W 1958 *Phys. Rev.* **109** 1492
[19] MacKinnon A and Kramer B 1993 *Rep. Prog. Phys.* **56** 1469
Lee A and Ramakrishnan T V 1985 *Rev. Mod. Phys.* **57** 287
[20] Abrahams E, Anderson P W, Licciardello D C and Ramakrishnan T V 1979 *Phys. Rev. Lett.* **42** 673
Gorkov L P, Larkin A I and Khmelnitskii D E 1979 *JETP Lett.* **30** 228
[21] Mirlin A D 2000 *Phys. Rep.* **326** 259
[22] Porter C E 1965 *Statistical Theory of Spectral Fluctuations* (New York: Academic)
[23] Efetov K B 1983 *Adv. Phys.* **32** 53
Efetov K B 1997 *Supersymmetry in Disorder and Chaos* (Cambridge: Cambridge University Press)
[24] Kravtsov V E and Mirlin A D 1994 *JETP Lett.* **60**
Falko V I and Efetov K B 1995 *Europhys. Lett.* **32** 627
Fyodorov Y V and Mirlin A D 1995 *Phys. Rev.* B **51** 13403
Fyodorov Y V and Mirlin A D 1995 *Phys. Rev.* B **52** 17413
Muzykantskii B A and Khmelnitiskii D E 1995 *Phys. Rev.* B **51** 5480
Fyodorov Y V and Mirlin A 1994 *Int. J. Mod. Phys.* B **8** 3795
Smolyarenko I and Altshuler B L 1997 *Phys. Rev.* B **55** 10451
[25] Ossipov A, Kottos T and Geisel T 2002 *Phys. Rev.* E **65** 055209
[26] Kottos T, Ossipov A and Geisel T 2003 *Phys. Rev.* E **68** 066215
[27] Uski V, Mehlig B, Römer R A and Schreiber M 2000 *Phys. Rev.* B **62** R7699
Uski V, Mehlig B and Schreiber M 2001 *Phys. Rev.* **63** 241101
Nikolić B 2001 *Phys. Rev.* B **64** 014203
[28] Shklovskii B I, Shapiro B, Sears B R, Lambrianides P and Shore H B 1993 *Phys. Rev.* B **47** 11487
[29] Alt'shuler B L and Shklovskii B I 1986 *Zh. Eksp. Teor. Fiz.* **91** 220
Alt'shuler B L and Shklovskii B I 1986 *Sov. Phys.—JETP* **64** 127
Aronov A G and Mirlin A D 1995 *Phys. Rev.* B **51** 6131
Kravtsov V E and Lerner I V 1995 *Phys. Rev. Lett.* **74** 2563
Zharekeshev I and Kramer B 1995 *Japan. J. Appl. Phys.* **34** 4361
[30] Stein J and Stöckmann H-J 1995 *Phys. Rev. Lett.* **75** 822
[31] Gräf H-D *et al* 1992 *Phys. Rev. Lett.* **69** 1296
Alt H *et al* 1995 *Phys. Rev. Lett.* **74** 62
[32] Kudrolli A, Kidambi V and Sridhar S 1995 *Phys. Rev. Lett.* **75** 822
[33] Pradhan P and Sridhar S 2000 *Phys. Rev. Lett.* **85** 2360
[34] Chalker J T, Kravtsov V E and Lerner I V 1996 *Pis. Zh. Eksp. Teor. Fiz.* **64** 355
Chalker J T, Kravtsov V E and Lerner I V 1996 *JETP Lett.* **64** 386
[35] Wegner F 1980 *Z. Phys.* B **36** 209
[36] Schreiber M and Grussbach H 1991 *Phys. Rev. Lett.* **67** 607
Parshin D A and Schober H R 1999 *Phys. Rev. Lett.* **83** 4590
Mildenberger A, Evers F and Mirlin A D 2002 *Phys. Rev.* B **66** 033109
[37] Evers F and Mirlin A D 2000 *Phys. Rev. Lett.* **84** 3690
Cuevas E, Ortuno M, Gasparian V and Perez-Garrido A 2002 *Phys. Rev. Lett.* **88** 016401
Varga I 2002 *Phys. Rev.* B **66** 094201
Varga I and Braun D 2000 *Phys. Rev.* **61** R11859
[38] Chalker J T and Daniell G J 1988 *Phys. Rev. Lett.* **61** 593
Huckestein B and Klesse R 1999 *Phys. Rev.* B **59** 9714
[39] Braun D, Hofstetter E, Montambaux G and MacKinnon A 2001 *Phys. Rev. Lett.* **64** 155107
Slevin K and Ohtsuki T 1999 *Phys. Rev. Lett.* **82** 382
Muttalib K A and Wölfle P 1999 *Phys. Rev. Lett.* **83** 3013
Markos P 1999 *Phys. Rev. Lett.* **83** 588

Shapiro B 1990 *Phys. Rev. Lett.* **65** 1510
[40] Cohen A, Roth Y and Shapiro B 1988 *Phys. Rev.* B **38** 12125
Soukoulis C M, Wang X S, Li Q M and Sigalas M M 1999 *Phys. Rev. Lett.* **82** 668
Slevin K and Ohtsuki T 1999 *Phys. Rev. Lett.* **82** 382
Muttalib K A and Wölfle P 1999 *Phys. Rev. Lett.* **83** 3013
Markos P 1999 *Phys. Rev. Lett.* **83** 588
[41] Sadreev A F and Rotter I 2003 *J. Phys. A: Math. Gen.* **36** 11413
[42] Schanz H 2003 *Physica* E **18** 429
Pichugin K, Schanz H and Seba P 2001 *Phys. Rev.* E **6405** 056227
Dittes F M 2000 *Phys. Rep.* **339** 216
[43] Savin D V, Fyodorov Y V and Sommers H-J 2005 *Proc. 2nd Workshop on Quantum Chaos and Localisation Phenomenon (Warsaw), Acta Phys. Pol. A* to be published (*Preprint* nlin.CD/0506040)
Fyodorov Y V, Savin D V and Sommers H-J 2005 *J. Phys. A: Math. Gen.* **38** 10731–60
[44] Wigner E P 1955 *Phys. Rev.* **98** 145
Smith F T 1960 *Phys. Rev.* **118** 349
[45] de Carvalho C A A and Nussenzveig H M 2002 *Phys. Rep.* **364** 83
[46] Aleiner I L, Brouwer P W and Glazman L I 2002 *Phys. Rep.* **358** 309
Alhassid Y 2000 *Rev. Mod. Phys.* **72** 895
[47] Raizen M, Salomon C and Niu Q 1997 *Phys. Today* **50** 30
Wiersma D S *et al* 1997 *Nature* **390** 671
Madison K W *et al* 1999 *Phys. Rev.* A **60** R1767
[48] Friedman N *et al* 2001 *Phys. Rev. Lett.* **86** 1518
Kaplan A *et al* 2001 *Phys. Rev. Lett.* **87** 274101
Milner V *et al* 2001 *Phys. Rev. Lett.* **86** 1514
[49] Baumert T *et al* 1991 *Phys. Rev. Lett.* **67** 3753
[50] Bacher G *et al* 1999 *Phys. Rev. Lett.* **83** 4417
Kumar R *et al* 1998 *Phys. Rev. Lett.* **81** 2578
[51] Chabanov A A *et al* 2003 *Phys. Rev. Lett.* **90** 203903
Skipetrov S E and van Tiggelen B A 2004 *Phys. Rev. Lett.* **92** 113901
Dal Negro L *et al* 2003 *Phys. Rev. Lett.* **90** 055501
Genack A Z *et al* 1999 *Phys. Rev. Lett.* **82** 715
[52] Savin D V and Sokolov V V 1997 *Phys. Rev.* E **56** R4911
[53] Casati G, Maspero G and Shepelyansky D L 1999 *Phys. Rev. Lett.* **82** 524
Casati G, Maspero G and Shepelyansky D L 2000 *Phys. Rev. Lett.* **84** 4088
Benenti G *et al* 2001 *Phys. Rev. Lett.* **87** 014101
[54] Ossipov A *et al* 2001 *Phys. Rev.* B **64** 224210
[55] Benenti G *et al* 2000 *Phys. Rev. Lett.* **84** 4088
Wimberger S *et al* 2002 *Phys. Rev. Lett.* **89** 263601
[56] Misirpashaev T S and Beenakker C W J 1998 *Phys. Rev.* A **57** 2041
[57] Patra M and Beenakker C W J 1999 *Phys. Rev.* A **60** 4059
Frahm K M, Schomerus H, Patra M and Beenakker C W J 2000 *Europhys. Lett.* **49** 48
Schomerus H, Frahm K M, Patra M and Beenakker C W J 2000 *Physica* A **278** 469
[58] Patra M 2003 *Phys. Rev.* E **67** 016603
Patra M 2003 *Preprint* cond-mat/0302506
[59] Fyodorov Y V and Mehlig B 2002 *Phys. Rev.* E **66** 045202
Fyodorov Y V and Sommers H-J 2003 *J. Phys. A: Math. Gen.* **36** 3303
[60] Cao H, Ling Y, Xu J Y and Burin A L 2002 *Phys. Rev.* E **66** 025601
[61] Apalkov V M, Raikh M E and Shapiro B 2004 *J. Opt. Soc. Am.* B **21** 132
Apalkov V M, Raikh M E and Shapiro B 2002 *Preprint* cond-mat/0212231
[62] Ossipov A, Kottos T and Geisel T 2003 *Europhys. Lett.* **62** 719
[63] Weiss M, Mendez-Bermudez A and Kottos T 2005 at press
[64] Borgonovi F, Guarneri I and Shepelyansky D 1991 *Phys. Rev.* A **43** 4517
[65] Titov M and Fyodorov Y V 2000 *Phys. Rev.* B **61** R2444
Terraneo M and Guarneri I 2000 *Eur. Phys. J.* B **18** 303
[66] Starykh O A, Jacquod P, Narimanov E and Stone A D 2000 *Phys. Rev.* E **62** 2078
[67] Pinheiro F A, Rusek M, Orlowski A and van Tiggelen B A 2004 *Phys. Rev.* E **69** 026605
[68] Kottos T and Weiss M 2002 *Phys. Rev. Lett.* **89** 056401
[69] Westervelt R M 1997 *Nano-Science and Technology* ed G Timp (New York: AIP)

[70] Kogan E, Mello P A and Liqun H 2000 *Phys. Rev.* E **61** R17
Beenakker C W J and Brouwer P W 2001 *Physica* E **9** 463
[71] Savin D V and Sommers H-J 2003 *Phys. Rev.* E **68** 036211
[72] Fyodorov Y V 2003 *JETP Lett.* **78** 250
[73] Misirpashaev T S and Beenakker C W J 1996 *JETP Lett.* **64** 319
Misirpashaev T S, Paasschens J C J and Beenakker C W J 1997 *Physica* A **236** 189–201
Paasschens J C J, Misirpashaev T Sh and Beenakker C W J 1996 *Phys. Rev.* B **54** 11887
[74] Ossipov A and Fyodorov Y V 2005 *Phys. Rev.* B **71** 125133
[75] Méndez-Sánchez R A *et al* 2003 *Phys. Rev. Lett.* **91** 174102
Kuhl U, Martínez-Mares M, Méndez-Sánchez R A and Stöckmann H-J 2004 *Preprint* cond-mat/0407197
[76] Jian Z, Pearce J and Mittleman D M 2003 *Phys. Rev. Lett.* **91** 033903
Pearce J, Jian Z and Mittleman D M 2003 *Phys. Rev. Lett.* **91** 043903
[77] Genack A Z, Sebbah P, Stoytchev M and van Tiggelen B A 1999 *Phys. Rev. Lett.* **82** 715
Chabanov A A and Genack A Z 2001 *Phys. Rev. Lett.* **87** 233903
[78] Gopar V A, Mello P A and Büttiker M 1996 *Phys. Rev. Lett.* **77** 3005
[79] Lewenkopf C H and Weidenmüller H A 1991 *Ann. Phys., NY* **212** 53
[80] Seba P, Zyczkowski K and Zakrewski J 1996 *Phys. Rev.* E **54** 2438
[81] Brouwer P W and Büttiker M 1997 *Europhys. Lett.* **37** 441
[82] Izrailev F, Saher D and Sokolov V V 1994 *Phys. Rev.* E **49** 130
[83] Brouwer P W, Frahm K M and Beenakker C W J 1997 *Phys. Rev. Lett.* **78** 4737
Sommers H-J, Savin D V and Sokolov V V 2001 *Phys. Rev. Lett.* **87** 094101
[84] Fyodorov Y V, Savin D V and Sommers H-J 1997 *Phys. Rev.* E **55** R4857
[85] Bouchaud J-P and Georges A 1990 *Phys. Rep.* **195** 127
[86] Texier C and Comtet A 1999 *Phys. Rev. Lett.* **82** 4220
[87] Ossipov A, Kottos T and Geisel T 2000 *Phys. Rev.* B **61** 11411
[88] Bolton-Heaton C J, Lambert C J, Falko V I, Prigodin V and Epstein A J 1999 *Phys. Rev.* B **60** 10569
[89] Jayannavar A M, Vijayagovindan G V and Kumar N 1989 *Z. Phys.* B **75** 77
Ramakrishna S A and Kumar N 1999 *Preprint* cond-mat/9906098
[90] Mendez-Bermudez J A and Kottos T 2005 *Phys. Rev.* B **72** 064108
[91] Mirlin A D, Fyodorov Y V, Dittes F-M, Quezada J and Seligman T H 1996 *Phys. Rev.* E **54** 3221
[92] Harper P G 1955 *Proc. Roy. Soc.* A **68** 874
Aubry S and Andre G 1980 *Ann. Isr. Phys. Soc.* **3** 133
Evangelou S N and Pichard J-L 2000 *Phys. Rev. Lett.* **84** 1643
Piéchon F 1996 *Phys. Rev. Lett.* **76** 4372
[93] Shechtman D, Blech I, Gratias D and Cahn J V 1984 *Phys. Rev. Lett.* **53** 1951
Kohmoto M, Kadanoff L P and Tang G 1983 *Phys. Rev. Lett.* **50** 1870
Luck J M and Petritis D 1986 *J. Stat. Phys.* **42** 289
Bellisard J, Iochum B, Scoppola E and Testard D 1989 *Commun. Math. Phys.* **125** 527
[94] Merlin R, Bajema K, Clarke R, Juang F Y and Bhattacharya P K 1985 *Phys. Rev. Lett.* **55** 1768
[95] Fujiwara T and Ogawa T 1990 *Quasicrystals* (Berlin: Springer)
[96] Gellermann W, Kohmoto M, Sutherland B and Taylor P C 1994 *Phys. Rev. Lett.* **72** 633
Hattori T, Tsurumachi N, Kawato S and Nakatsuka H 1994 *Phys. Rev.* B **50** 4220
[97] Geisel T, Ketzmerick R and Petschel G 1991 *Phys. Rev. Lett.* **66** 1651
Geisel T, Ketzmerick R and Petschel G *Quantum Chaos Between Order and Disorder* ed J Casati and B Chirikov (Cambridge: Cambridge University Press) pp 634–59
[98] Kuhl U and Stöckmann H-J 1998 *Phys. Rev. Lett.* **80** 3232
[99] Steinbach F, Ossipov A, Kottos T and Geisel T 2000 *Phys. Rev. Lett.* **85** 4426
Ossipov A, Weiss M, Kottos T and Geisel Theo 2001 *Phys. Rev.* B **64** 224210
[100] Ghulinyan M, Oton C J, Dal Negro L, Pavesi L, Sapienza R, Colocci M and Wiersma D S 2005 *Phys. Rev.* B **71** 094204
Dal Negro L, Oton C J, Gaburro Z, Pavesi L, Johnson P, Lagendijk A, Righini R, Colocci M and Wiersma D S 2003 *Phys. Rev. Lett.* **90** 055501